Iranian Journal of Medical Physics

ijmp.mums.ac.ir

Assessment of Internal and External Surrogates for Lung Stereotactic Body Radiation Therapy

Milovan Savanovic[1,2*], Bojan Strbac[3], Drazan Jaros[4], Dejan Cazic[4], Goran Kolarevic[4], Jean-Noël Foulquier[1]

1. Faculty of Medicine, University of Paris-Saclay, 94276 Le Kremlin-Bicêtre, France.
2. Department of Radiation Oncology, Tenon Hospital, 75020 Paris, France.
3. MATER Private Hospital, Physics department, Eccles Street, Dublin 7, Ireland.
4. Affidea, International Medical Centers, Center for Radiotherapy, 78000 Banja Luka, Bosnia and Herzegovina.

ARTICLE INFO

Article type:
Original Paper

Article history:
Received: Jun 03, 2020
Accepted: Aug 14, 2020

Keywords:
Lung Cancer
Motion
Surrogate Marker
Four-Dimensional Computed Tomography
Stereotactic Body Radiotherapy

ABSTRACT

Introduction: In this study, we aimed to evaluate internal (lung, heart and diaphragm) and external (nine glass marbles) marker motion in correlation with lung tumor motion and determine potential surrogate for respiratory gating radiation therapy (RGRT) depending on tumor localization, upper lobe (UL) versus lower lobe (LL).

Material and Methods: We included 58 patients (34 male and 24 female) with small lung cancer (≤ 5cm), who underwent stereotactic body radiation therapy (SBRT). All patients were scanned and contoured in all ten phases (Varian Eclipse 13.7) after four-dimensional computed tomography simulation (4D-CT). The motions of internal and external markers were analyzed and correlated with tumor motion. Pearson correlation coefficient (PCC) was used to evaluate the correlation between internal and external marker motion and tumor motion.

Results: The median (range) values of tumor motion were 3.2 (0.6-11.0) and 8.6 (4.0-24.0) mm in the UL and LL, respectively. The median (range) values of organs motion and PCC comparing UL vs. LL were 2.0 (0.3-9.1) vs. 6.0 (2.8-13.9) mm and 0.46 (0.30-0.95) vs. 0.79 (0.50-0.94) for the lung, respectively, 11.9 (2.5-16.3) vs. 12.5 (5.0-22.5) mm and 0.68 (0.11-0.93) vs. 0.89 (0.30-0.99) for the diaphragm, respectively, and 3.9 (2.5-6.3) vs. 7.6 (4.5-8.6) mm and 0.49 (0.20-0.70) vs. 0.59 (0.36-0.83) for the heart, respectively. The external marker motion and correlation coefficient for UL and LL were 2.5 (0.9-7.4) vs. 2.3 (1.0-5.9) mm and 0.54 (0.09-0.96) vs. 0.73 (0.27-0.94), respectively.

Conclusion: Lung and diaphragm motion correlate better with tumor motion than the external marker. Diaphragm motion can be an excellent indicator for treatment based on RGRT.

►*Please cite this article as:*
Savanovic M, Strbac B, Jaros D, Cazic D, Kolarevic G, Foulquier JN. Assessment of Internal and External Surrogates for Lung Stereotactic Body Radiation Therapy. Iran J Med Phys 2021; 18: 352-360. 10.22038/IJMP.2020.50131.1820.

Introduction

In modern radiation therapy, lung cancer is treated with high conformal doses to expose gross tumor volume (GTV) with steep dose gradients, protecting surrounding healthy tissues [1]. Precise delivery of high conformal doses controls tumor progression and reduces toxicity to the organs at risk (OAR), including the heart, esophagus, and spinal cord [2]. Better protection of OARs can be obtained by using an accelerator equipped with image-guided radiation therapy (IGRT) and/or using techniques such as respiratory gating radiation therapy (RGRT) or tumor tracking [3]. However, the treatment can be impacted by tumor motion due to respiration, heartbeat, or movement of the gastrointestinal tract [4].

The tumor in a lung cancer patient is mobile because of the patient's respiration, and it can move up to several centimeters, depending on localization [5]. Therefore, monitoring of the organs in motion is facilitated with the development of the image guided technique and with the implementation of fiducial markers in or near the tumor during radiation therapy [6-8]. Generally, patients refuse the implementation of fiducial markers because the transthoracic implementation of fiducials has been associated with considerable risk of iatrogenic pneumothorax due to unpleasant experience with biopsy [9, 10].

External and fiducial markers are used in lung tumor tracking. The model of tumor motion is created from the correlation of external markers with orthogonal stereoscopic images of fiducials implanted in or near the target volume, using the Synchrony Respiratory Tracking System (Accuray Oncology, Sunnyvale, CA). This model allows the robotic linear accelerator Cyber Knife (Accuray Oncology, Sunnyvale, CA) to follow the target and account for the movement of tumors or healthy tissue [10].

The amplitude of the tumor and internal and external markers motion depend on the imaging

*Corresponding Author: Tel: +33644802626; Email: milovan_savanovic@yahoo.com

system used, which can be performed in the static computed tomography (CT), single-photon emission computed tomography (SPECT), positron emission tomography (PET), magnetic resonance imaging (MRI), and dynamic (fluoroscopy, ultrasound, and 4D-CT) modes. The static imaging mode represents a snapshot of the patient's anatomy at a specific moment, while the dynamic imaging mode allows presentation of tumor and internal (fiducial and OARs) and external markers motion within the respiratory cycle, which can impact on image reconstruction [11]. To facilitate image reconstruction, an immobilization system and/or breathing methods, such as deep inspiration breath hold (DIBH) or abdominal compression, may be employed to take into consideration patient motion and motion induced by respiration[4, 12].

To evaluate the correlation between internal and external markers motion with tumor motion, different surrogates, such as diaphragm motion, lung volume, and external marker, were used [13-16]. The surrogates were used to investigate tumor motion prediction to perform the treatment based on RGRT or tumor tracking.

The aim of this study was to use a non-invasive method to find the correlation between lung tumor motion and internal marker motion (lung motion, diaphragm motion, and heart motion) and external marker motion (glass marbles) and to evaluate potential surrogate for treatment based on RGRT for lung SBRT patients.

Materials and Methods

Patient Selection

Retrospectively, this study was conducted on a consecutive cohort of patients, between March 2017 and June 2019, from a single institution. The cohort initially included 60 lung cancer patients (35 males and 25 females) with a small tumor volume (≤ 5cm). The patients' selection was based on the following inclusion and exclusion criteria: the general state of the patients, their respiratory status, and patient body mass, and unbearable pain in certain positions. Only two patients from the group of 60 were excluded from this study. One male patient was excluded due to a respiratory problem and having a breathing amplitude that was not sufficiently large to be captured with a charged-couple device (CCD) camera. One female patient was excluded due to her body mass (stereotactic body frame could not be positioned) and pain in the shoulder when she had arms raised above the head. The primary analysis was conducted on 58 lung cancer patients (i.e., 34 males and 24 females).The patient characteristics are presented in Table 1.

In this patient cohort, we did not have any patients with cancer localized in the middle lobe.

Data Acquisition

All patients were scanned in supine position with arms above the head and performed free breathing (FB) using a GE Light speed CT (General Electric Medical Systems, Waukesha, WI) equipped with an Real-Time Position Management system (RPM, Varian Medical Systems, Palo Alto, CA, USA). Monitoring of the patients' breathing was performed using an infrared CCD camera mounted on the treatment couch, and it captured motion of the reflective block marker placed over the xiphoid process.

Table 1. Patients' main characteristics with number. Percentage, minimum and maximum values were mentioned in parenthesis

Characteristics	Number (range or percentage)
Number of patients	58
Age	68 (56 – 90)
Gender	
Male	34 (59 %)
Female	24 (41 %)
Tumor location	
Upper lobe	35 (60 %)
Left lobe	12 (34 %)
Right lobe	23 (66 %)
Lower lobe	23 (40 %)
Left lobe	5 (22 %)
Right lobe	18 (78 %)
GTV volume	
Upper lobe (cc)	2.3 (0.4 – 16.5)
Lower lobe (cc)	2.4 (0.5 – 11.9)
Breathing cycle (s)	3.8 (2.1 – 7.6)
4D-CT scan time (s)	36 (29 – 57)

Abbreviations: GTV – gross tumor volume, 4D-CT four-dimensional computed tomography.

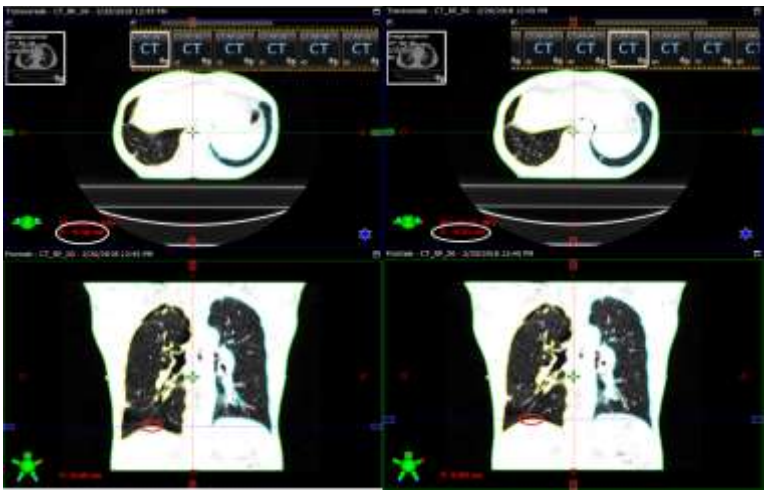

Figure 1. Measurement of diaphragm motion for right cupola between 0% and 50% phases for this particular patient

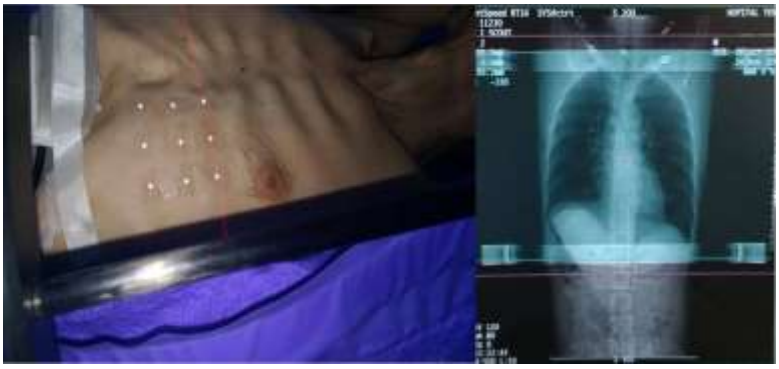

Figure 2. Simulation of SBRT patient with BlueBag BodyFIX system immobilization and using nine glass marbles (external markers) attached by adhesive tape to the patient's thorax and in level with the tumor

The patients were prepared for two helical CTs (with and without stereotactic body frame) and one 4D-CT acquisition according to the institutional protocols. Patients with small tumor volume (≤ 5cm) were immobilized in a supine position with arms above their head in the BlueBAG BodyFIX system immobilization (Medical Intelligence, Schwabmünchen, Germany).

The acquisition parameters for the helical CTs and the 4D-CT were: 0.7 s/rotation period, 120 kVs, mA ranged from 10 to 440 mA, automatic exposure control (AEC) was turned on, 16 slices detector, and slice thickness of 1.25 mm (the beam collimation width was 20 mm).

Internal Marker Motion

Lung Motion

Lung motion caused by respiration depends on the anatomical structure of the lungs, left versus the right lung. The right lung (yellow) with three lobes has a bigger volume than the left lung (cyan) with two lobes (Figure 1). Since lung cancer is part of the lung, it is supposed that lung motion causes tumor motion during respiration. To determine lung motion and its correlation with tumor motion, the lungs (left and right) were contoured automatically through all the ten phases of respiratory cycle, in Varian Eclipse 13.7 version, and the contours were retouched manually.

Diaphragm Motion

Diaphragm motion was measured from the coronal plane, where marker line (red circle) was positioned on the top of the cupola of the diaphragm (either the right or the left cupola). The position value of cupola motion was read on the axial plane (white circle) for all the phases and for both cupolas (Figure 1). The numerical difference between the phases, reading on the axial plane, represents diaphragm motion through the respiratory cycle.

Heart Motion

Involuntary motion involves movements of the organs such as those caused by the heart and respiratory motion. Respiratory-induced heart motion impacts image acquisition and may greatly degrade the effectiveness of treatment [17, 18]. Tumor-organ proximity and tumor motion can increase toxicity, delivering a higher dose to the heart [19]. Even though heart motion is poorly evaluated in radiotherapy in general, the impact of heart contribution on tumor motion derives the tumor from its main trajectory, known as the effect of hysteresis [20]. By studying heart motion, it let us know to what extent the heart can influence the treatment and if the heart can be used as a surrogate for lung SBRT treatment. To determine heart

motion and heartbeat through all the ten phases of the respiratory cycle, the heart was contoured in Varian Eclipse 13.7 treatment planning system (TPS). The contouring of the heart was performed in accordance with the guidelines published by the Radiation Therapy Oncology Group (RTOG) consensus guidelines [21].

External Marker Motion

Our study with the external marker was performed because lung cancer treatment commonly correlates internal tumor motion with external marker motion (Varian block marker or Cyber Knife synchrony vest with fiber optic tracking markers) and/or surface monitoring [4, 22]. Knowing that lung tumors have a complex direction of tumor motion (SI direction, elliptical and hysteresis) induced by respiration (which includes diaphragm motion and heart contribution), a larger area of the thorax should be covered with markers [23]. During simulation, we used glass marbles as the external marker (Figure 2).

Nine glass marbles, with a diameter of 3 mm, were attached to the patient's thorax vertically and horizontally by using adhesive tape (Figure 2), depending on tumor localization (UL or LL). For the vertical axis, we used anatomical lines: the parasternal line, the midclavicular line, and the anterior axillary line. The distance between the horizontal lines was 2.5 cm.

Placing several markers on the patient's thorax ensured by the close proximity of at least one marker to the tumor, covering the entire trajectory of tumor motion, regardless of direction. Also, several external markers allowed us to evaluate thoracic surface deformation during patient respiration and determine the potential correlation between one or more external markers with internal tumor motion.

Data Analysis

After 4D-CT simulation, contouring was performed for the tumor structure, lung, heart, and all the nine external markers in all the ten phases and in the Varian Eclipse 13.7 treatment planning system (TPS). The trajectory of each volume of interest contouring in all of the ten phases was evaluated from the center of mass, using statistic tools from DICOM (Digital Imaging and Communications in Medicine) images. The magnitude of the 3D radius vector $\left\|\vec{r}\right\|$ represents the overall motion that was calculated from the coordinates in each direction:

$$\left\|\vec{r}\right\| = \sqrt{x^2 + y^2 + z^2} \quad (1)$$

Where *x*, *y*, and *z* are the latero-lateral (LL), anterior-posterior (AP), and superior-inferior (SI) directions, respectively.

The data regarding tumor motion, internal markers (lung, diaphragm and heart) motion and external markers motion was analyzed depending on tumor localization (UL vs. LL), taking into consideration that diaphragmatic motion is higher in the LL than in the UL. The correlation between lung tumor motion and internal and external markers motion was analyzed by the Pearson correlation coefficient (PCC).

Statistical analysis was performed using GraphPad Prism 7.00 version (SD, California, and USA). Tumor motion was compared to the internal and external marker motion between the UL and LL, using unpaired *t*-test. Also, PCC was compared between the UL and LL, using another unpaired *t*-test. Data was considered statistically significant at $p < 0.05$.

The results are presented as median and range values because large outliers lead to a large skew in mean values.

Results

The median values and their ranges of tumor motion, internal markers (the diaphragm, lung, and heart) motion, and external marker (glass marble) motion, depending on tumor localization (UL vs. LL) are presented in Table 2. The PCCs are presented as correlation of tumor motion with all of the markers.

The overall tumor motion was greater than 10 mm (ranging from 10.9 mm to 24.0 mm) for eight patients, greater than 5 mm (ranging from 5.1 mm to 9.2 mm) for 13 patients, and only two patients had a tumor motion less than 5 mm (4.0 mm and 4.4 mm) in the LL. This is contrary to the UL, where overall tumor motion was less than 5 mm (ranging from 0.9 mm to 4.9 mm) for 29 patients, two patients had motion greater than 5 mm (6.1 mm and 7.1 mm), and four patients had motion greater than 10 mm (ranging from 10.1 mm to 11 mm).

Table 2. Results of tumor motion, lung motion, diaphragm motion, heart motion, and external marker motion, with PCC presented with median value and their range

Parameters	UL (mm)	PCC UL	LL (mm)	PCC LL	p*	p+
Tumor	3.2 (0.6–11.0)	-	8.6 (4.0–24.0)	-	<0.001	
Lung	2.0 (0.3–9.1)	0.46 (0.30–0.95)	6.0 (2.8–13.9)	0.79(0.50–0.94)	<0.001	<0.001
Diaphragm	11.9 (2.5–16.3)	0.68 (0.11–0.93)	12.5 (5.0–22.5)	0.89(0.30–0.99)	=0.616	<0.005
Heart	3.9 (2.5–6.3)	0.49 (0.20–0.70)	7.6 (4.5–8.6)	0.59(0.36–0.83)	<0.05	=0.736
Ext mar	2.5 (0.9–7.4)	0.54 (0.09–0.96)	2.3 (1.0–5.9)	0.73 (0.27–0.94)	=0.403	<0.01

Abbreviations: UL – upper lobe, LL – lower lobe, PCC – Pearson correlation coefficient, p* - p-value calculated for motion between UL and LL, p+ - p-value calculated for PCC between UL and LL, Ext mar – external marker.

The amplitude of left lung motion (5.6 [1.2-13.9] mm) was greater than the amplitude of right lung motion (2.0 [0.3-9.5] mm) ($p<0.05$). Lung motion was less than 10 mm in the UL for all the patients, while PCC was higher than 0.70 for eight patients (ranging from 0.74 to 0.94), of which four patients had PCC (ranging from 0.91 to 0.95) higher than 0.90. Three patients had lung motion greater than 10 mm (ranged from 10.4 mm to 13.9 mm), while16 patients had PCC (ranging from 0.72 to 0.94) higher than 0.70, including seven patients with PCC (ranging from 0.91 to 0.94) higher than 0.90 in the LL.

The same median values were obtained for both cupola of diaphragm motion, 12.5 (2.5-22.5) mm in the left and 12.5 mm (6.2-16.3) in the right cupola ($p=0.339$). Only one patient had diaphragm motion greater than 20 mm (22.5 mm). The PCC was (ranging from 0.71 to 0.99) higher than 0.70 for 18 patients, of which 11 patients had PCC (ranging from 0.91 to 0.99) higher than 0.90 in the LL. In detail, eight patients had PCC (ranged from 0.72 to 0.93) higher than 0.70and three patients had PCC (ranged from 0.91 to 0.93) greater than 0.90 in the UL.

Maximum heart motion was 8.6mm in the LL, while PCC was higher than 0.70 only for four patients (ranged from 0.71 to 0.83), with maximum PCC of 0.83 for one patient. Heartbeat was found at every two phases (variation in x and y components of heart motion up to 2 mm every two phases).

External marker motion was greater than 5 mm for four patients (ranging from 5.6 mm to 7.4 mm) in the UL and one patient (5.9 mm) in the LL. Ten patients had PCC (ranging from 0.71 to 0.96) higher than 0.70 in the UL (only one patient had PCC [0.96] higher than 0.90), while14 patients had PCC (ranging from 0.72 to 0.94) higher than 0.70 in the LL (two patients had PCC [0.91 and 0.94] higher than 0.90).

The results of the diaphragm motion are presented in Table 3. The maximum values of the diaphragm motion within the respiratory cycle are presented with bold values.

In six different cases, maximum expansion immobilized the diaphragm between four to five phases, depending on the patient's respiration.

Internal motion of the tumor and external motion of the external marker are presented in Figure 3 based on the lobe. The trajectories of tumor motion and external marker motion are presented in the UL (Figure 3[a] and [b]) and LL (Figure 3[c] and [d]).

Table 3. Diaphragm motion (mm) within the entire respiratory cycle for six different cases. Bold values correspond to maximum displacement of the diaphragm.

Phase (%)	Phases with maximum diaphragm motion (mm)					
	20-50%	30-60%	30-70%	40-70%	50-80%	90-20%
0	9.82	3.60	2.98	7.75	7.48	2.70
10	9.70	2.98	2.48	7.75	7.35	2.70
20	8.82	2.35	2.23	7.50	6.85	2.70
30	8.82	1.98	1.48	7.25	5.73	2.08
40	8.82	1.98	1.48	7.00	5.48	1.57
50	8.82	1.98	1.48	7.00	5.35	1.20
60	9.20	1.98	1.48	7.00	5.35	1.95
70	9.33	2.35	1.48	7.00	5.35	2.33
80	9.70	2.23	2.23	7.25	5.35	2.33
90	9.82	3.35	2.98	7.75	6.23	2.70

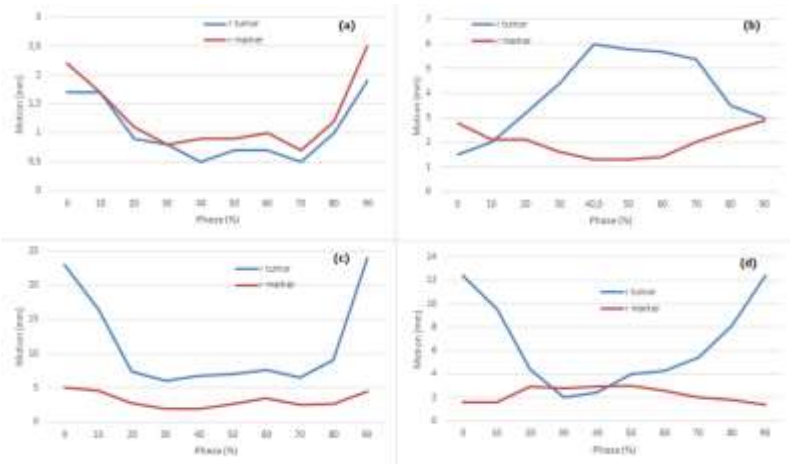

Figure 3. External marker motion (red line) and internal tumor motion (blue line) were presented depending on the UL (a) and (c) vs. LL (b) and (d) without and with time shift

Evaluating tumor and marker motion between referent scan (helical CT without stereotactic body frame) and all phases of the respiratory cycle, we found a time shift in both lobes for 19 patients in the UL (Figure 3 [b]) and 11 patients in the LL (Figure 3[d]).

Discussion

In this study, 58 lung cancer patients with small tumor volume underwent SBRT treatment. The authors examined the correlation between lung tumor motion and the internal markers motion (i.e., lung, diaphragm, and heart motion) and external markers motion (nine glass marbles), depending on the lobe (UL vs. LL).

Comparing median values of tumor motion, we found that tumor motion was three times greater in the LL than in the UL ($p<0.001$). Analyzing the amplitude of tumor motion between UL vs. LL, we found that tumors moved more than 5 mm in 6% vs. 57%, while 14% vs. 35% moved more than 10 mm. Similar results were found in the study of Liu et al., where about 40% of lung tumors moved more than 5 mm and about 12% moved more than 10 mm [24].

Better correlation between tumor motion and internal and external markers was found in the LL rather than in the UL, while higher PCC occurred for the diaphragm (0.89), rather than the lung (0.79), external marker (0.73), and finally, the heart (0.59).

The amplitude of left lung motion was 2.8 times greater than the amplitude of right lung motion ($p<0.05$). Ehrhardt et al. found that motion was 1.2 greater in the right lung than in the left lung [25]. Analyzing lung motion between the UL and LL, we noted that lung motion was three times larger in the LL rather than the UL ($p<0.001$). A greater difference (4.1 times) was found in the Fayad et al. study, performed with a small patients' cohort (ten patients) [26].

The results of lung motion may justify the difference in results of tumor motion according to tumor localization (UL vs. LL). We found lung motion to be three times and tumor motion 2.7 times greater in the LL, rather than in the UL. This can be explained from an anatomical standpoint, taking into account the sponginess of lung tissues. In the LL, lung motion was impacted by diaphragm motion, which is associated with chest wall expansion in the lower part of the thorax during free breathing, allowing for larger motion. In the UL, lung motion was reduced due to the limitation of the chest wall expansion, which was immobile during free breathing, while the lungs were compressed by diaphragm motion, increasing density and decreasing elasticity in the UL. These effects impacted the tumor motion in the UL, reducing their amplitude.

With greater tumor motion, we obtained better correlation (PCC), about 1.7 times higher in the LL rather than in the UL ($p<0.01$). In 70% of the patients, PCC was greater than 0.70, and 30% had a PCC higher than 0.90 in the LL, comparing to 23% with PCC higher than 0.70 and 11% higher than 0.90 in the UL. Lung motion with high PCC value can be used as a surrogate for tumor motion.

The diaphragm moves during respiration, like other organs located in the abdomen. The amplitude of diaphragm motion was not significant ($p=0.339$) between the left and right cupola. A smaller difference (less than 5% difference) was found comparing diaphragm motion between lobes (UL and LL) ($p<0.005$). Similar results regarding diaphragm motion (13 mm) were obtained in the Weiss et al. study, using fluoroscopy imaging (30 patients) and in Korin et al. study using magnetic resonance imaging (MRI) for 15patients [27, 28].

However, the amplitude of diaphragm motion was greater than the amplitude of tumor motion in both lobes, 73% in the UL ($p<0.005$) and 31% in the LL ($p<0.001$), whereas tumor motion had a greater amplitude than diaphragm motion in 14% of patients with tumors located in the LL. In the Liu et al. study, diaphragm displacement (16.5 mm) was greater than tumor motion (13.6 mm) in the SI direction, which was highly correlated with diaphragm motion [24].

A higher PCC was found in the LL (26%) rather than the UL (<0.005). The PCC was higher than 0.70 for 23% vs. 78% of patients, while 11% vs. 48% of patients had PCC higher than 0.90, comparing the UL with the LL.

In the studies of Vedam et al. and Mageras et al., diaphragm motion and external marker motion were used for the potential surrogate for lung tumor motion [14, 29]. They found a strong correlation (ranging from 0.79 to 0.95) between the external marker motion and diaphragm motion. Cervino et al. evaluated the correlation between diaphragm motion and lung tumor motion in the superior-inferior direction, using fluoroscopic images from ten patients [30]. They obtained the strong correlation factors of 0.94 and 0.98 for a simple linear model and a more complex linear model, respectively. These differences may be due to different imaging techniques and smaller patient cohorts in cited studies.

Analyzing diaphragm motion, we found that the diaphragm was motion less during several phases (4 to 5 phases) within the respiratory cycle, which corresponds to the stability of tumor motion at end-expiration and end-inspiration (Table 3) [5]. Diaphragm motion may confirm the choice of gated window for RGRT technique, which allows for a reduction in treatment volume and a better sparing of the OARs from the high dose delivered during SBRT treatment. It appears that diaphragm motion (stability) may be used as a surrogate for treatment based on RGRT.

Greater heart motion (49%) ($p<0.05$) and higher PCC (17%) ($p=0.736$) were found in the LL rather than in the UL. Comparing median values, we found that the heart motion amplitude was 18% greater than the amplitude of tumor motion in the UL, contrary to the LL where tumor motion was 11% greater than heart motion amplitude. In the Rasheed et al. study, heart motion was 15% greater than tumor motion [31].

Heartbeat and heart motion affect tumor motion, creating motion with hysteresis in 32% of patients,

enlarging treatment volume and decreasing PCC. In the study of Seppenwoolde et al., 30% of patients had tumor motion with hysteresis due to heartbeat [20]. These motions with hysteresis impact on PCC between tumor motion and internal and external markers. Only 10% of patients had PCC higher than 0.70 between heart motion and tumor motion. It is not advisable to use the heart as a surrogate during treatment delivery due to a lower PCC and heartbeat contribution within heart motion.

Also, heart motion can impact on simulation and treatment delivery, escalating the dose to the heart for treatment based throughout the entire respiratory cycle (ITV volume). Cardiac toxicity can also be affected by heart motion, overlapping heart structure with treatment volume during irradiation and escalating the dose to the heart. The RGRT technique may be used to reduce heart volume from treatment volume and spare the heart from high doses, while the DIBH technique can be used to freeze heart motion during treatment, reducing the dose to the heart [32, 33].

The external marker (glass marble) motion was greater in the UL (10%) than in the LL (p=0.403). External marker motion was greater than 5 mm in 9% of patients. The amplitude of tumor motion was higher than the amplitude of external marker motion in both lobes, 22% in the UL ($p<0.001$) vs. 73% in the LL ($p<0.005$). On the other hand, a larger PCC (26%) was found in the LL ($p<0.01$). The PCC between tumor and external marker motion was higher than 0.70 for 29% in the UL vs. 61% in the LL, which means that a difference in motion amplitude does not affect the PCC between the tumor and the external marker. Decreased PCC values were found when trajectories of tumor and external marker motion mismatched. In Figure 3, trajectories of tumor motion (blue line) and external marker motion (red line) are presented within all phases of the respiratory cycle in the UL (Figure 3[a] and [b]) and the LL (Figure 3[c]and [d]). When the helical CT scan without stereotactic body frame was acquired without a time shift, the trajectories of tumor and external marker motion matched, having the same shape and increasing PCC (Figure 3[a] and [c]). The PCC values still depend on amplitude and localization of the tumor and external marker. In the case of time shift (Figure 3[b] and [d]), the trajectories of tumor and external marker motion mismatched, decreasing PCC values. A better correlation was obtained between the tumor and the nearest marker to the tumor in all the patients.

We concluded that the correlation coefficient strongly depends on the respiratory phase during which the helical CT scan without stereotactic body frame was acquired, the shape of tumor motion and external marker motion, as well as their localization and time shift (Figure 3). A similar conclusion was found in the study of Gierga et al.[15]. They found that tumor motion (25 mm) was larger than external marker motion (2 to 9 mm), while correlation depended on the tumor's position compared to the external marker position.

A better correlation with tumor motion may be obtained using an inserted fiducial marker. When fiducial markers were inserted near the tumor, uncertainties due to time shift were excluded. However, the remaining key problems are localization and distance between the tumor and fiducial marker. Smith et al. reported that the correlation coefficient may be impacted when the distance between tumor motion and the fiducial marker increases [34]. The use of fiducial markers is limited because it can lead to complications such aspneumothorax, focal intrapulmonary hemorrhage, hemoptysis, mild hemothorax, gas embolism, and death [8, 35].

The correlation between tumor motion and the internal and external markers may strongly affect the imaging technique, which can generate images with poor quality, polluted by artifacts [11]. Structure delineation based on poor image quality may underestimate or overestimate the tumor, internal (fiducial and OARs) and external marker volumes, location, and motion, creating overlap between structures [36]. Using an adequate imaging technique and/or breathing methods (DIBH and abdominal compression) may take into consideration or reduce the motion induced by respiration [4]. On the other hand, an adequate system immobilization ensures precise and comfortable patient positioning, reducing inter- and intra-fraction motion [12].

The best solution was to treat mobile tumors without surrogates, which can be done by using a recently developed magnetic resonance imaging-guided linear accelerator (MRI-LINAC). However, the use of the MRI-LINAC was limited by the availability of MRI scanners, limited familiarity with MRI in radiotherapy, and medical contraindications to MRI [37].

Conclusion

In this study, the correlation between lung tumor motion and internal (lung, heart and diaphragm) and external markers was investigated. Better correlation was found in the LL for all markers, internal and external.

Lung tumors and internal markers moved without time shift, which allowed for higher PCC. The diaphragm had greater motion and higher PCC than the lung and heart. The diaphragm motion (stability between phases) can be used as a surrogate to perform the RGRT technique, which allows for a reduction in treatment volume and better sparing of the OARs. Even though the heart had greater amplitude of motion than the lung, PCC was higher for the lung. It is not advisable to use the heart as a surrogate because of a lower PCC and heartbeat contribution. The lung may be used as a surrogate, but lung motion strongly depends on the general state of the patient, the lung physiology, and the patient's respiratory problems.

The correlation of tumor motion and external marker motion depends on the distance between the tumor and marker, the shape of the tumor and marker motion, time shift, and the patient's breathing. Also, heartbeat and heart motion can provide tumor motion with hysteresis,

which impacts on the correlation coefficient between tumor motion and external marker motion.

References

1. Giraud P, Elles S, Helfre S. Conformal radiotherapy for lung cancer: different delineation of the gross tumor volume (GTV) by radiologists and radiation oncologists. Radiother Oncol. 2002 Jan;62(1):27-36.
2. De Ruysscher D, Faivre-Finn C, Moeller D. European Organization for Research and Treatment of Cancer (EORTC) recommendations for planning and delivery of high-dose, high precision radiotherapy for lung cancer. Radiother Oncol. 2017 Jul;124(1):1-10.
3. Goyal S, Kataria T. Image guidance in radiation therapy: techniques and applications. Radiol Res Pract. 2014;2014:705604.
4. Keall PJ, Mageras GS, Balter JM, Emery RS, Forster KM, et al. The management of Respiratory Motion in Radiation Oncology report of AAPM Task Group 76. Med Phys. 2006 Oct;33(10):3874-900.
5. Korreman SS. Image-guided radiotherapy and motion management in lung cancer. Br J Radiol. 2015 Jul;88(1051):20150100.
6. Das SK, Ten Haken RK. Functional and Molecular Image Guidance in Radiotherapy Treatment Planning Optimization. Semin Radiat Oncol. 2011 Apr; 21(2): 111-8.
7. Sterzing F, Engenhart-Cabillic R, Flentje M, Debus J. Image-Guided Radiotherapy. A New Dimension in Radiation Oncology. Dtsch Arztebl Int. 2011 Apr; 108(16):274-80.
8. Jung IH, Song SY, Jung J. Clinical outcome of fiducial-less CyberKnife radiosurgery for stage I non-small cell lung cancer. Radiat Oncol J. 2015 Jun; 33(2):89-97.
9. Kollmeier MA, Bochner B. Intravesical Fiducial Marker Placement to Facilitate Image-Guided Radiation Therapy for Patients With Muscle-Invasive Bladder Cancer. UroToday Int J. 2011 Feb; 4(1):art16.
10. Schroeder C, Hejal R, Linden PA. Coil spring fiducial markers placed safely using navigation bronchoscopy in inoperable patients allows accurate delivery of CyberKnife stereotactic radiosurgery. J Thorac Cardiovasc Surg. 2010 Nov; 140(5):1137-42.
11. Wanet M, Sterpin E, Janssens G, Delor A, Lee JA, Geets X. Validation of the mid-position strategy for lung tumors in helical TomoTherapy. Radiother Oncol. 2014;110(3):529-37.
12. Hubie C, Shaw M, Bydder S, Lane J, Waters G, Mc Nabb M, et al. A rondomised comparison of three different immobilisation devices for thoracic and abdominal cancers. J Mec Radiat Sci. 2017 Jun; 64(2):90-6.
13. Nankali S, Torshabi AE, Miandoab PS, Baghizadeh A. Investigation on Performance Accuracy of Different Surrogates in Real Time Tumor Tracking at External Beam Radiotherapy. Frontiers in Biomedical Technologies. 2015; 2(2):73-9.
14. Vedam SS, Kini VR, Keall PJ, et al. Quantifying the predictability of diaphragm motion during respiration with a noninvasive external marker. Med Phys. 2003 Apr; 30(4):505-13.
15. Gierga DP, Brewer J, Sharp GC. The correlation between internal and external markers for abdominal tumors: Implications for respiratory gating. Int J Radiat Oncol Bio Phys. 2005; 61(5):1551-8.
16. Lee SY, Lim S, Ma SY, Yu J. Gross tumor volume dependency on phase sorting methods of four-dimensional computed tomography images for lung cancer. Radiat Oncol J. 2017 Sep;35(3):274-80.
17. Ablitt NA, Gao J, Keegan J, Stegger L, Firmin DN, Yang GZ. Predictive cardiac motion modeling and correction with partial least squares regression. IEEE Trans Med Imaging. 2004 Oct;23(10):1315-24.
18. George R, Keall PJ, Kini VR. Quantifying the effect of intrafraction motion during breast IMRT planning and dose delivery. Med Phys. 2003 Apr;30(4):552-62.
19. Wang X, Pan T, Pinnix C, Zhang SX. Cardiac motion during deep-inspiration breath-hold: implications for breast cancer radiotherapy. Int J Radiat Oncol Biol Phys. 2012 Feb 1;82(2):708-14.
20. Seppenwoolde Y, Shirato H, Kitamura K. Precise and real-time measurement of 3D tumor motion in lung due to breathing and heartbeat, measured during radiotherapy. Int J Radiat Oncol Biol Phys. 2002 Jul 15;53(4):822-34.
21. Radiation therapy oncology group. Atlases for organs at risk (OARs) in thoracic radiation therapy. 2011. available from: https://www.rtog.org/CoreLab/ContouringAtlases/LungAtlas.aspx.
22. Wijenayake U, Park SY. Real-Time External Respiratory Motion Measuring Technique Using an RGB-D Camera and Principal Component Analysis. Sensors (Basel). 2017 Aug 9;17(8).
23. Mageras GS, Pevsner A, Yorke ED. Measurement of lung tumor motion using respiration-correlated CT. Int J Radiat Oncol Biol Phys. 2004 Nov 1;60(3):933-41.
24. Liu HH, Balter P, Tutt T. Assessing Respiration-Induced Tumor Motion and Internal Target Volume Using Four-Dimensional Computed Tomography for Radiotherapy of Lung Cancer. Int J Radiat Oncol Biol Phys. 2007;68(2):531–40.
25. Ehrhardt J, Werner R, Schmidt-Richberg A, Handels H. Statistical modeling of 4D respiratory lung motion using diffeomorphic image registration. IEEE Trans Med Imaging. 2011 Feb;30(2):251-65.
26. Fayad H, Pan T, Clement JF, Visvikis D. Technical note: Correlation of respiratory motion between external patient surface and internal anatomical landmarks. Med Phys. 2011 Jun;38(6):3157-64.
27. Weiss PH, Baker JM, Potchen EJ. Assessment of hepatic respiratory excursion. J Nucl Med. 1972 Oct;13(10):758-9.
28. Korin HW, Ehman RL, Riederer SJ, Felmlee JP,Grimm RC. Respiratory kinematics of the upper abdominal organs: a quantitative study. Magn Reson Med 1992 Jan;23(1):172–8.
29. Mageras G, Torke E, Rosenzweig KE. Fluoroscopic evaluation of diaphragmatic motion reduction with a respiratory gated radiotherapy system. J Appl Clin Med Phys. 2001;2:191–200.
30. Cervino LI, Chao AK, Sandhu A, Jiang SB. The diaphragm as an anatomic surrogate for lung tumor motion. Phys Med Biol. 2009 Jun 7;54(11):3529-41.
31. Rasheed A, Jabbour SK1, Rosenberg S. Motion and volumetric change as demonstrated by 4DCT: The effects of abdominal compression on the GTV, lungs, and heart in lung cancer patients. Pract Radiat Oncol. 2016 Sep-Oct;6(5):352-9.

32. De La Fuente Herman T, Vlachaki MT, Herman TS, Hibbitts K, Stoner JA, Ahmad S. Stereotactic body radiation therapy (SBRT) and respiratory gating in lung cancer: dosimetric and radiobiological considerations. J Appl Clin Med Phys. 2010 Jan 29;11(1):3133.
33. Mani KR, Bhuiyan A, Alam M. Dosimetric comparison of deep inspiration breath hold and free breathing technique in stereotactic body radiotherapy for localized lung tumor using Flattening Filter Free beam. Polish Journal of Medical Physics and Engineering. 2018;24(1):15-24.
34. Smith RL, Yang D, Lee A, Mayse ML, Low DA, Parikh PJ. The correlation of tissue motion within the lung: implications on fiducial based treatments.Med Phys. 2011 Nov;38(11):5992-7.
35. Bhagat N, Fidelman N, Durack JC. Complications associated with the percutaneous insertion of fiducial markers in the thorax. Cardiovasc Intervent Radiol. 2010 Dec;33(6):1186-91.
36. Dou TH, Thomas DH, O'Connell D, Bradley JD, Lamb JM, Low DA. Technical Note: Simulation of 4DCT tumor motion measurement errors. Med Phys. 2015;42(10):6084-9.
37. Pathmanathan AU, van As NJ, Kerkmeijer LGW. Magnetic Resonance Imaging-Guided Adaptive Radiation Therapy: A "Game Changer" for Prostate Treatment?. Int J Radiat Oncol Biol Phys. 2018;100(2):361-73.